Theoretical investigation of the residual electrical resistivity concentration dependence of transuranium metal alloys

Yu. Yu. Tsiovkin,* A. V. Lukoyanov, A. A. Povzner, and E. S. Koneva
Ural State Technical University–UPI, 19 Mira Street, 620002 Ekaterinburg, Russia

M. A. Korotin, A. O. Shorikov, and V. I. Anisimov
Institute of Metal Physics, Ural Division, Russian Academy of Sciences, 18 Sofia Kovalevskaya Street, 620041 Ekaterinburg GSP-170, Russia

A. N. Voloshinskii
Moscow State Institute of Radio Engineering, Electronics, and Automation, 78 Vernadsky Avenue, 119454 Moscow, Russia

V. V. Dremov
Russian Federal Nuclear Center, Institute of Technical Physics, 13 Vasiliev Street, Snezinsk, Chelabinnsk Region, Russia
(Received 4 June 2009; revised manuscript received 5 October 2009; published 30 October 2009)

A many-band conductivity model has been derived and applied to analyze the concentration dependence of the electrical residual resistivity (RR) of several actinides based disordered alloys. It was qualitatively shown that equal probabilities of $s \rightarrow d$ and $s \rightarrow f$ transitions of scattered conductivity electrons lead to the deviations from Nordgeim's rule observed in these alloys. Numerical evaluation of RR of neptunium, plutonium, americium, and curium based alloys was made within the coherent potential approximation (CPA) derived for the many-band conductivity model. Numerical calculations were made using *ab initio* obtained bcc-Np and fcc-Pu, Am, and Cm densities of states, as the starting point for the iterative CPA procedure. The results of the RR modeling were compared with available experimental data and allow us to conclude that the proposed model offers promising opportunities to investigate RR of similar classes of alloys.

DOI: 10.1103/PhysRevB.80.155137 PACS number(s): 71.10.−w, 71.15.−m, 71.27.+a

I. INTRODUCTION

Electrical resistivity of actinide metals and alloys has been investigated experimentally for a rather long time due to the complexity of the problem.[1–5] At normal conditions pure Np and Cm demonstrate metallic type of temperature dependencies of electrical resistivity with characteristic value at room temperature about 60–140 $\mu\Omega\cdot$cm.[2,5] On the other hand, Am, which is an ordinary metal at ambient pressure with slightly enhanced electrical resistivity $\sim$70 $\mu\Omega\cdot$cm, shows a striking growth of the resistivity almost of an order of magnitude up to 500 $\mu\Omega\cdot$cm during the transition into orthorhombic structure at the pressures above 16 GPa.[3,4,6] Moreover, the negative temperature coefficient of electrical resistivity at high temperature was found in some δ-Pu dilute alloys.[1,7–10] With regard to above mentioned, some ordinary kinetic and magnetic properties observed in transuranium metals look rather anomalous. One can suppose that these anomalies originate mostly from peculiarities of their electronic ground state.

Basing on calculated electronic ground-state properties of Np, Pu, Am, and Cm, a number of well-known anomalies in temperature dependencies of electrical resistivity of Pu-based dilute alloys as well as ordinary metallic type of electrical resistivity of pure Np, Cm, and Am was explained.[11,12] Mott's two-band conductivity model combined with the coherent potential approximation (CPA) allowed analyzing this problem from the most general point of view. It follows from these calculations that initial ground state of 5f-electron behavior in actinides does not affect electrical resistivity response of these metals, which is determined mostly by evolution of the density-of-states (DOS) curve at the Fermi level with temperature.

It is a well-known fact that electronic structure of alloy differs significantly from that of initial pure metals. In this paper we study how this modification of the electronic structure influences the electrical residual resistivity (RR) and other kinetic and magnetic properties of actinides concentrated alloys.

The RR of actinide based alloys (AcBAs) was investigated experimentally in Np-Pu[2] and Am-Pu[4] systems. The characteristic values of the RR are about 100÷150 $\mu\Omega\cdot$cm, which exceed those for 3d-5d transition-metal based alloys (TMBAs). Such high values of the RR for AcBA could be explained qualitatively within the Mott two-band conductivity model.[13] In this model, the value of resistivity is determined by the value of DOS of appropriate conductivity band at the Fermi level. These values in actinide's d and f bands surpass significantly those in 3d-5d metals and the RR behavior in AcBA and TMBA is different. In TMBA the RR value slightly depends on concentration of alloy components, whereas essential shift of the RR maximum from equal concentrations point was observed in AcBA.

In the case of TMBA, the nature of such a shift was explained using the assumption that the DOS of the alloy at the Fermi level is a weighted average of DOSs of alloy components. It was shown that accounting for the difference between d-band DOS values at the Fermi level of alloy components and using Nordgeim rule the RR maximum is always shifted toward metal with the larger value of DOS at

the Fermi level.[14] However, perturbation-theory calculation of RR concentration dependencies for actinides alloys is not valid, due to nonsmall intensity of electron-impurity interaction. Moreover, self-consistent procedure is necessary to reproduce specific feature of electrons scattering and realistic concentration dependencies of RR in real alloys.

The anomalies in electrical resistivity behavior in the Pu-based dilute alloys and ordinary temperature dependence of pure Np, Pu, Am, and Cm were explained within an ordinary Mott two band conductivity model without any assumptions concerning intensity of electron-impurity and electron-phonon interactions, using *ab initio* calculated DOS of metals. Similar approach could be useful to understand the RR concentration dependencies in the concentrated disordered alloys of artificial metals. However, in the general case, only many-band conductivity model is suitable, because (i) transitions of $(s+p)$-electrons into almost empty d and f bands have equal probabilities and (ii) the values of electrons coupling are different for various $(s+p)$, d, and f bands in concentrated alloys.

Modern investigations indicate quasimetallic behavior of $5f$ electrons in Th, U, and Np. On the other hand, in heavy actinides (Am, Cm, Bk, and Cf) $5f$ electrons are almost localized. Plutonium takes a significant place in this series and demonstrates an intermediate behavior of $5f$ electrons with the increase in localization induced by α-δ transition.

The DOS and other ground-state properties of solid states can be determined by modern numerical calculations, based on the density-functional theory.[15] For example, the standard local (spin) density approximation with accounting for Hubbard (U) interaction [L(S)DA+U] allows one to reproduce well the ground-state properties of many compounds except the plutonium and metals beyond it in the Periodic Table.[16] The problem arises due to comparable strength of spin-orbit coupling (SOC) (about 1 eV for Pu) and exchange (Hund's) interaction (about 0.5 eV).

Recently, correct treatment of both Coulomb repulsion and spin-orbit interaction in rotation invariant form allowed to describe a nonmagnetic ground state of fcc-Pu with six $5f$ electrons with almost filled $J=5/2$ subband and almost empty $J=7/2$ one.[16–19] Ground-state properties of other actinides at normal conditions were calculated elsewhere.[6,19–21]

Numerous band methods based on the density-functional theory have been applied to investigate the electronic structure of plutonium. Approving a well-known fact that the DFT can correctly reproduce experimental crystal structures, a phase diagram of plutonium was found in good agreement with experiment.[18,22] Investigations carried out in frame of the LDA+U+SO method demonstrated that the nonmagnetic ground state of plutonium is provided by $J=0$ total moment and can easily be broken.[16] This conclusion agrees well with the result of the "around-the-mean-field" version of LDA+U.[17] The resulting DOS shows that the spin-orbit coupling leads to sufficiently separated fulfilled $j=5/2$ subband, which is located just below the Fermi level, and almost empty $j=7/2$ subband, which is shifted due to strong Coulomb interaction to 3–4 eV above the Fermi level. This result is determined by the f^6 configuration of the plutonium f shell. Recent experiments revealed f^5 configuration in δ-plutonium.[23] Better agreement with experiment can be found in other calculations.[22,24] The review of the problem could be found elsewhere.[16,19,25,26]

The LDA+U+SO method has been chosen as a starting point and resulted DOSs of actinides under consideration were used for CPA simulations. The CPA approach allows modeling DOS of a disordered alloy for various concentrations of components and does not require cumbersome supercells as it would be needed in the alternative approach of supercells.

In this paper we present at first, the derivation of many-band CPA equations and some qualitative results of RR model calculations of actinide alloys. Then, starting from results of numerical simulations for bcc-neptunium, fcc-plutonium and americium,[16,19] and fcc-curium,[12] the RR concentration dependence in their alloys was analyzed from the most general point of view, in terms of CPA for the many-band conductivity model. The complex structure of d, f electron DOSs, and their deformation due to electron-impurity interactions have been accounted. Thus we have avoided some debatable models and any assumptions concerning the features of DOS near the Fermi level as well as assumptions about the weakness of interaction.

II. MODEL AND MANY BAND CPA EQUATIONS

Let us consider the $s(p)$, d, and f electrons performing intraband and interband transitions (without spin flips) as a result of scattering at Coulomb fields of randomly distributed ions of alloy components. We take into account that probabilities of interband scattering of $s(p)$ conductivity electrons ($s \rightarrow d$ and $s \rightarrow f$) are proportional to DOSs values at the Fermi level of corresponding bands. Moreover these values are comparable. Hence we assume that (i) $s(p)$ conductivity electrons perform mainly interband transitions $s \rightarrow d$ and $s \rightarrow f$, (ii) accepted d or f bands are partially filled. According to the conditions, let us consider a Hamiltonian, describing systems of $s(p)$, d, and f electrons,

$$\hat{H} = \hat{H}_0 + \hat{V},$$

$$\hat{H}_0 = \sum_l E_l a_l^+ a_l,$$

$$\hat{V} = \frac{1}{N} \sum_{n,l,l'} e^{-i(\vec{k}-\vec{k}',\vec{R}_n)} B_{l,l'} a_l^+ a_{l'}, \tag{1}$$

where E_l is a periodical part of total energy of an electron with the quantum number l, including band index $j(j=s(p),d,f)$, and wave vector $\vec{k}$; $\vec{R}_n$ is a radius vector of the nth site of a crystal lattice,

$$B_{l,l'}(n) = \nu(n)[\lambda_{\vec{k}j,\vec{k}'j}\delta_{j,j'} + \lambda_{\vec{k}j,\vec{k}'j'}(1-\delta_{j,j'})]. \tag{2}$$

Factor $\nu(n)=\alpha_A(n)c_B-\alpha_B(n)c_A$ describes ions of alloy components randomly distributed over the sites of a crystal lattice, $\alpha_{A(B)}(n)=1$ if the site number n is occupied by an ion of the sort $A(B)$, and it equals to zero in another case. Intensities of intraband and interband transitions of electrons are described by parameters λ_{ll} and $\lambda_{ll'}$, respectively.

The s, p, d, and f bands overlap and therefore hybridization effects have to be taken into account. However, it is well known that they lead only to renormalization of the electron ground-state Hamiltonian and do not change its scattering part. Realistic DOSs of actinides used in our calculations take into account the hybridization effects of $s(p)$, d, and f bands that enables us to take them into consideration in $\hat{H}_0$ and for simplicity we keep the same band names after renormalization.

We derive the equations for many-band CPA using the condition of diagonality of the shift operator in the $\hat{H}_0$ representation. Hence, total resolvent of the full energy operator $\hat{H}$ is

$$\hat{R} = (z - \hat{H})^{-1}. \tag{3}$$

The diagonal part of the total resolvent $\hat{R}$ in the $\hat{H}_0$ representation is

$$\hat{G} = (z - \hat{H}_0 - \hat{\Delta})^{-1}, \tag{4}$$

where $\hat{\Delta}$ is a diagonal operator (in the $\hat{H}_0$ representation)

$$\hat{\Delta} = \frac{1}{N}\sum_{n,l,l'} e^{-i(\vec{k}-\vec{k}',\vec{R}_n)}\Delta_j \delta_{jj'} a_l^+ a_l. \tag{5}$$

The real part of coherent potential Δ_j determines the shift η_j, and its imaginary part γ_j determines the broadening of single-electron levels.

Using the Dyson equation

$$\hat{R} = \hat{G} + \hat{G}(\hat{V} - \hat{\Delta})\hat{R}, \tag{6}$$

a scattering operator $\hat{T}$ can be determined in convenient form as

$$\hat{R} - \hat{G} = \hat{G}\hat{T}\hat{G}. \tag{7}$$

Multiplying the right and left sides of Eq. (7) by $\hat{G}^{-1}$, the following expression for the scattering operator is obtained:

$$\hat{T} = \hat{G}^{-1}(\hat{R} - \hat{G})\hat{G}^{-1}. \tag{8}$$

This expression determines the order of matrix products and allows one to avoid difficulties associated with the choice of right- or left-matrix products. Using the Dyson Eq. (6) and expression (8), we obtain the following operator series:

$$\hat{\Delta} = [(\hat{V} - \hat{\Delta})\hat{G}(\hat{V} - \hat{\Delta}) + (\hat{V} - \hat{\Delta})\hat{G}(\hat{V} - \hat{\Delta})\hat{G}(\hat{V} - \hat{\Delta}) + \cdots]_{diag}. \tag{9}$$

The *diag* index means that only diagonal part of the sum of operator products in the $\hat{H}_0$ representation should be taken. It was shown in Ref. 27, that the series (9) has reciprocally compensated terms, containing the shift operator in indirect form. Excluding these compensated terms from expression (9), one obtains finally the shift operator

$$\hat{\Delta} = [\hat{V}\hat{G}\hat{V} + \hat{V}\hat{G}\hat{V}\hat{G}\hat{V} + \ldots]_D = \hat{V}\hat{G}\hat{V}(1 - \hat{G}\hat{V})^{-1}. \tag{10}$$

The D index means that in $[\ldots]_D$ all diagonal terms in the $\hat{H}_0$ representation are kept and these compensated items are already omitted.

Summation (10) can be performed conveniently in a matrix form. Since the $\hat{G}$ and $\hat{\Delta}$ operators are diagonal in the H_0 representation, we determine Green's functions F, the coherent potential $\hat{\Delta}$,

$$F = \begin{bmatrix} F_s & & \\ & F_d & \\ & & F_f \end{bmatrix}, \quad \Delta = \begin{bmatrix} \Delta_s & & \\ & \Delta_d & \\ & & \Delta_f \end{bmatrix}, \tag{11}$$

and interaction V, where we consider λ_{ll} and $\lambda_{ll'}$ as independent on $\vec{k}$ and $\vec{k}'$ wave vectors

$$V = \begin{bmatrix} B_{ss} & B_{sd} & B_{sf} \\ B_{ds} & B_{dd} & B_{df} \\ B_{fs} & B_{fd} & B_{ff} \end{bmatrix}. \tag{12}$$

Here

$$F_j = \frac{1}{N}\sum_{\vec{k}} \frac{1}{(z - E_{\vec{k},j} - \Delta_j)} \tag{13}$$

is the Green's function of an electron in the jth band.

Within single-electron and single-site approaches and notations (5, 11–13), the series (10) is summed up accurately with the following condition: $|F_j\lambda_{jj'}| < 1$.

Band-structure calculation shows that the value of partial DOSs of d and f electrons at the Fermi level in actinides is much higher than that of $s(p)$ electrons. Therefore, it is reasonable to assume that in pure actinide metals and their alloys $|\lambda_j F_s| \ll 1$ and $|\lambda F_s| \ll 1$, which means that $s(p)$ conductivity electrons perform mainly interband transitions $s \to d$ and $s \to f$. Using this simplification, the result of summation of the matrix series for $\Delta_j (j = s, d, f)$ could be written as follows:

$$\Delta_s = \frac{1}{A}\sum_{j \neq j'} \{B_{sj}F_jB_{js}(1 - F_{j'}B_{j'j'}) + B_{sj}F_jB_{jj'}F_{j'}B_{j'j}\}, \tag{14}$$

$$\Delta_j = \frac{1}{A}\{B_{jj}F_jB_{jj}(1 - F_{j'}B_{j'j'}) + B_{jj'}F_{j'}B_{j'j}(1 + F_jB_{jj})\}, \tag{15}$$

where

$$A = (1 - F_dB_{dd})(1 - F_fB_{ff}) - B_{df}F_fB_{fd}F_d. \tag{16}$$

Note, that the entire system of CPA equations could be derived in the same way, without any simplifications. However, its analysis would not give any new significant or important result.

Averaging Eqs. (14) and (15) over configuration, denoting $\lambda_{jj} = \lambda_j$ for coherent potentials for s, d, and f bands, one obtains the following system:

$$\Delta_s = \sum_{j\neq j'} c_A \frac{(c_B\lambda_{sj})^2 F_j[1-c_B\lambda_{j'}F_{j'}]+(c_B)^3\lambda F_j F_{j'}}{[1-c_B\lambda_d F_d][1-c_B\lambda_f F_f]-(c_B\lambda_{df})^2 F_d F_f} + c_B \frac{(c_A\lambda_{sj})^2 F_j[1+c_A\lambda_{j'}F_{j'}]-(c_A)^3\lambda F_j F_{j'}}{[1+c_A\lambda_d F_d][1+c_A\lambda_f F_f]-(c_A\lambda_{df})^2 F_d F_f}, \quad (17)$$

$$\Delta_d = c_A \frac{(c_B\lambda_d)^2 F_d[1-c_B\lambda_f F_f]+(c_B\lambda_{df})^2 F_f[1+c_B\lambda_d F_d]}{[1-c_B\lambda_d F_d][1-c_B\lambda_f F_f]-(c_B\lambda_{df})^2 F_d F_f} + c_B \frac{(c_A\lambda_d)^2 F_d[1+c_A\lambda_f F_f]-(c_A\lambda_{df})^2 F_f[1-c_A\lambda_d F_d]}{[1+c_A\lambda_d F_d][1+c_A\lambda_f F_f]-(c_A\lambda_{df})^2 F_d F_f}, \quad (18)$$

where $\lambda=\lambda_{sd}\lambda_{sf}\lambda_{df}$. The equation for coherent potential of f electrons could be obtained from Eq. (18) replacing band indexes $f\leftrightarrow d$.

Neglecting interband transitions, i.e., $\lambda=0$ as follows from Eqs. (17) and (18), three independent equations corresponding to the single-band model of CPA could be written,

$$\Delta_j = c_A \frac{(c_B\lambda_j)^2 F_j}{1-c_B\lambda_j F_j} + c_B \frac{(c_A\lambda_j)^2 F_j}{1+c_A\lambda_j F_j}. \quad (19)$$

In the case of the single-band model, Eq. (19) for coherent potential differs from the Soven CPA equation[28] since the latter was obtained assuming that the average of single-site scattering matrix T over configurations is zero, $\langle T_n\rangle_{conf}=0$.

In the second order of perturbation theory in the weak-coupling limit for s electrons the following result could be written:

$$\Delta_s^{(2)} = \sum_j B_{jj}^2 F_j. \quad (20)$$

Note, that the terms in the third order are

$$\Delta_s^{(3)} = \sum_{j,(j\neq j')} (B_{sj}F_j B_{jj} + B_{sj'}F_{j'}B_{j'j})F_j B_{js}. \quad (21)$$

These are the products of the Green's functions of d and f electrons, which is important for accurate calculation of RR.

Equations (17) and (18) contain a number of parameters describing intraband and interband couplings. Within the framework of CPA, parameters of intraband coupling are usually assumed to be equal to the difference in gravity centers of bands of corresponding alloy components. These parameters could be extracted from partial DOS obtained in *ab initio* band-structure calculations. Since all these parameters depend on each other, only one parameter $\lambda\approx 1/2(\lambda_d+\lambda_f)$ can be used as a free parameter.

III. DOS OF ALLOYS USED IN CPA

The use of *ab initio* calculated DOS as the starting point for CPA equations allows one to take into account features of electronic structure of the alloy components and describe the alloy kinetic properties in a reliable way. The usual assumption for the initial DOS of alloys used in CPA is average weighted model. Nothing could be said about physical validity of this model. However, it seems reasonable to use charge conservation law for calculation of initial alloy DOS.

Let us assume that the number of occupied states n in each band of alloy is equal to average weighted number of occupied states of components

$$n_j = \sum_{\alpha=A,B} c_\alpha n_{\alpha,j}. \quad (22)$$

As the maximum number of f, d, and s electrons in each subband is limited due to normalization of DOS, the same expression can be written for empty states,

$$\bar{n}_j = \sum_{\alpha=A,B} c_\alpha \bar{n}_{\alpha,j}. \quad (23)$$

Since the number of electrons in a band is defined by DOS function of components $g^\alpha(E)$, the following expressions for occupied and empty states can be written, respectively:

$$\int_{E_{0j}}^{E_F} g_j(E)dE = \sum_{\alpha=A,B} c_\alpha \int_{E_{\alpha,0j}}^{E_{F,\alpha j}} g_{\alpha,j}(E)dE;$$

$$\int_{E_F}^{E_{c,j}} g_j(E)dE = \sum_{\alpha=A,B} c_\alpha \int_{E_{F,\alpha}}^{E_{\alpha,cj}} g_{\alpha,j}(E)dE, \quad (24)$$

where E_F and $E_{F,\alpha}$ are the Fermi energies, $E_{\alpha,0j}$ are the energies of the bottom of the jth band, and E_{cj}, $E_{\alpha,cj}$ are the cutoff energies of DOS of alloy and its components, respectively. The Fermi energy can be determined requiring DOS continuity at E_F.

Solving Eqs. (24), one obtains expressions for the alloy DOS,

$$g_j(E) = \sum_\alpha c_\alpha \frac{E_{F,\alpha,j}-E_{\alpha,0j}}{E_F-E_{0j}} g_{\alpha j}\left(\frac{E_{F,\alpha}-E_{\alpha,0j}}{E_F-E_{0j}}(E-E_{0j})+E_{\alpha,0j}\right)$$

for $E\leq E_F$

and

$$g_j(E) = \sum_\alpha c_\alpha \frac{E_{\alpha,cj}-E_F}{E_{cj}-E_{F,\alpha}} g_{\alpha j}\left(\frac{E_{\alpha,cj}-E_{F,\alpha}}{E_{cj}-E_F}(E-E_F)+E_{F,\alpha}\right)$$

for $E\geq E_F$. (25)

From the same requirement (DOS continuity) the equation can be deduced,

$$\sum_\alpha c_\alpha \frac{E_{F,\alpha}-E_{\alpha,0}}{E_F-E_0} g_\alpha(E_{F,\alpha}) = \sum_\alpha c_\alpha \frac{E_{\alpha,c}-E_F}{E_c-E_F} g_\alpha(E_{F,\alpha}). \quad (26)$$

Solution of the later gives the Fermi energy of alloy:

$$\frac{E_F-E_0}{E_c-E_F} = \frac{\Sigma_\alpha c_\alpha (E_{F,\alpha}-E_{\alpha,0}) g_\alpha(E_{F,\alpha})}{\Sigma_\alpha c_\alpha (E_{\alpha,c}-E_{F,\alpha}) g_\alpha(E_{F,\alpha})}. \quad (27)$$

Using the Leman representation

$$F(z) = \int_{-\infty}^{+\infty} \frac{g(E)dE}{z-E}, \quad (28)$$

the initial Green's function of alloy can be found. This procedure parameterizes the problem completely. Then partial

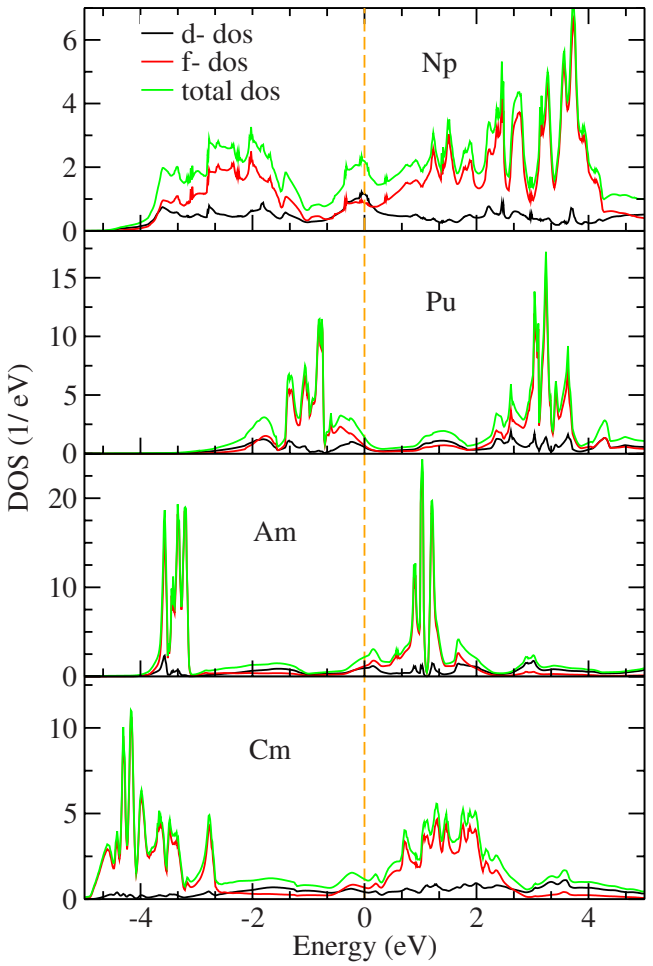

FIG. 1. (Color online) Results of LDA+U+SO calculations of partial d- and f-DOS and total DOS of the bcc-Np, fcc-Pu, Am, and Cm metals. The Fermi level is set to zero.

LDA+U+SO DOSs of pure metals are used to calculate alloy DOS and solve of system of CPA Eqs. (25)–(27) numerically.

IV. RESULTS AND DISCUSSION

A. DOS of actinides

Neptunium in bcc phase is stable from 600 K until 644 K with f^4 electronic configuration and have a lattice constant a=3.488 Å. Plutonium in the fcc phase also known as δ-Pu is stable from 594 K until 725 K and has a lattice constant a=4.637 Å. Above 925 K or at 6.1(2) GPa Am metal undergoes the transition into fcc phase with[29] a=4.613 Å. At high temperature or high pressure about 17(2) GPa Cm metal also transforms into fcc phase.[20] In the present calculation for curium metal the value a=4.47293 Å was used.

The obtained from the LDA+U+SO calculations DOS curves for all metals are presented in Fig. 1. For plutonium, americium, and curium they were discussed previously[12,16,19] in detail. In the calculations we set the same Coulomb U value equal to 2.5 eV for all pure metals, which gives correct equilibrium volume for δ-Pu.[16] The Hund exchange parameters were calculated using "constrained LDA" procedure[30] and was found to be 0.48 eV for Np, Pu, and Am, and 0.52 eV for Cm.

In Fig. 1(a) the LDA+U+SO calculated DOS for neptunium metal is presented. Based on the calculated occupancies in jj- and LS-coupling scheme, one can conclude that the intermediate coupling scheme is more appropriate to present LDA+U+SO partial DOSs for neptunium. The occupation numbers in jj-coupling scheme are $n_{5/2}$=3.13 and $n_{7/2}$=1.14. The calculated value of the effective magnetic moment was found to be μ_{eff}^{calc}=7.79 μ_B, which is in good agreement with the experimental data.[31]

Note that although both Pu and Am could be described well in frames of jj-coupling scheme and found to have the same f^6 configuration with zero total moment, the obtained DOS differs drastically. For both Pu and Am j=5/2 subband is occupied and j=7/2 subband is almost empty. But whereas the Fermi level cuts the top of occupied j=5/2 subband in the case of Pu, in the Am case it cuts the bottom of empty j=7/2 subband. The center of gravity of j=5/2 subband is positioned near 1 eV and 3.5 eV below the Fermi energy in Pu and Am, respectively.

Curium has f^7 configuration and effective magnetic moment about $7\mu_B$ which lies within the range of available magnetic-moment values from experiment.[31] In curium, a filled subband lies below the Fermi level from −5 eV to −2.5 eV and a broad empty subband is positioned just above the Fermi level up to 3 eV, see Fig. 1(c). In contrast to Pu and Am, where the jj-coupling scheme is valid and the occupied bands (j=5/2) contain 6f electrons, in Cm some intermediate coupling scheme close to LS type is appropriate.[18] As a consequence of this, 7f electrons of Cm are located in an occupied subband presenting a mixture of bands with different orbital character. Thus the occupied subbands of Am and Cm seem similar, but their orbital character is substantially varied.

B. Residual resistivity: qualitative results

Preliminary qualitative result of RR calculations of actinides alloys could be found in frames of perturbation theory. In the second order of perturbation theory $\rho \sim \mathrm{Im}\,\Delta_s$ which means that

$$\rho^{(2)} \sim c_A c_B \sum_j \lambda_j^2 \mathrm{Im} F_j|_{E=E_F} \tag{29}$$

This leads to an ordinary Nordgeim-like result of the RR concentration dependence with maximum at concentration equal to 0.5. It was shown previously for the case of ordinary 3d-5d-transition-metal alloys,[14] that simple model of average weighted DOS can provide correct position of the RR maximum. The maximum is always shifted to metal with the larger DOS value at the Fermi level in good agreement with experimental data for all 3d-5d transition-metal alloy. However, in case of actinide alloys this simple rule can often be violated due to both many-band type of conductivity and high scattering intensity.

Actually, one can see from Eqs. (20) and (21) that the sum of the second and third order terms of perturbation theory for resistivity gives

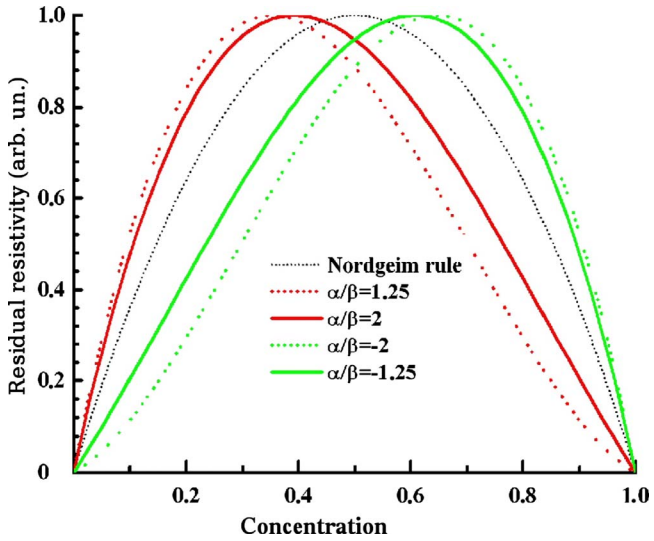

FIG. 2. (Color online) Comparison of the model RR calculation results for various values of the ratio $\alpha/\beta(\alpha=\Sigma_j\lambda_j^2\ \mathrm{Im}\ F_j)$ and the Nordgeim curve.

$$\rho^{(2+3)} \sim c_A c_B \sum_j [\lambda_j^2\ \mathrm{Im}\ F_j + (c_B^2 - c_A^2)\cdot\beta_j], \tag{30}$$

where

$$\beta_j = [2\lambda_{sj}^2\lambda_{jj}\ \mathrm{Im}\ F_j\ \mathrm{Re}\ F_j + \lambda_{sj}\lambda_{jj'}\lambda_{j's}(\mathrm{Re}\ F_j\ \mathrm{Im}\ F_{j'} + \mathrm{Re}\ F_{j'}\ \mathrm{Im}\ F_j)]_{E=E_F}. \tag{31}$$

Concentration dependence of the second term in Eq. (30) is responsible for the shift of the RR maximum and determines through the value of β_j and sign of $\lambda_{jj'}\lambda_{j'j''}\lambda_{j''j}\ \mathrm{Re}\ F_j$ (the values of $\mathrm{Re}\ F_j$ and $\mathrm{Im}\ F_{j'}$ can be obtained at the Fermi level). Since the real part of Green's function of real alloys is a rapidly changing function of energy, one cannot predict position of RR maximum in actinides alloys from this simplified consideration. However, results of this model calculation of RR with fixed values of $\mathrm{Im}\ F_{j'}(E_F)$, $\mathrm{Re}\ F_{j'}(E_F)$, and $|\lambda_{jj}|=|\lambda_{jj'}|$ are presented in Fig. 2 can be useful for understanding of possible types of RR concentration dependencies. One can see that RR curves calculated with Eq. (30) differs from Nordgeim's parabola and the change in $\mathrm{Re}\ F_{j'}(E_F)$ sign leads to the shift of RR maximum. The value of the shift could be determined using a ratio of the first and second terms in expression (30). Moreover, one can see from Fig. 2 that type of the RR behavior changes significantly and several quasilinear intervals of the RR curve appear.

From the qualitative analysis given above one can conclude that accounting for some orders of perturbation series results in significant modification of the Nordgeim curve. Hence, all such approximations and omissions of terms should be seriously justified. The model of RR proposed in this paper [Eqs. (17) and (18)] avoids this problem because of the full summation of the series (9).

C. Residual resistivity: numerical results

Kubo formula for diagonal part of conductivity tensor was used to calculate realistic alloy RR,

$$\sigma = (\rho)^{-1} = \sum_{j,\sigma} \frac{2e^2\hbar n_j}{3\pi^2} \int dE g_j(E) E \times \left[\frac{\gamma_j^\sigma(\zeta)}{(\zeta - E - \eta_j^\sigma(\zeta))^2 + (\gamma_j^\sigma(\zeta))^2}\right]^2. \tag{32}$$

Equation (32) was derived replacing the matrix element of the squared speed of electron with average kinetic energy: $(\vartheta_x^2 \approx 2\bar{E}/m)$.[14] Nevertheless this rather rough approximation has no effect on final result since RR concentration dependencies obtained with different values of this matrix element, or calculated within various approximations, are almost the same. Apparent limitations on validity of Eq. (32) arise due to the neglecting of back transitions $f(d) \rightarrow s$ of conductivity electrons. This transition should be taken into account only if the ratio of DOS values of $f(d)$ and s bands at the Fermi level is large.

As it was mentioned above, it is convenient to use the difference between gravity centers of $5f$ bands of alloy components as this parameter and to define λ_{dd} using initial DOS of compound. Moreover, we use $\lambda_{jj'}=1/2(\lambda_{jj}+\lambda_{j'j'})$ approximations for the intensities of interband transitions. Note that relative positions of DOSs of alloy components at the total-energy scale are unambiguously fixed by λ_{ff} parameters of theory. The values of parameters λ_{ff} for Pu and Am were obtained from the best fitting of the theoretical curves to available experimental data in Figs. 4 and 6 as 2.65 eV and 5.37 eV, respectively. Using Np gravity center as zero on total-energy scale, the defined value of parameter λ_{ff} for Cm was found to be 6.7 eV. This set of parameters was used in all calculations.

1. Residual resistivity of Np-based alloys

Neptunium is a metal with quasimetal type of $5f$-electron behavior and its alloys with other later actinides are of great interest due to nonordinary evolution of kinetic properties expected for different concentrations of the alloys components. The main cause of this interest is a local minimum in RR of α-phase Np-Pu alloys found at Np concentration $10\div20\%$.[2] The nature of this unusual behavior of RR is still unclear. Our calculations allows suggesting that this minimum is attributed to the changes in the DOS value at the Fermi level.

The results of our CPA calculations for Np-Pu DOSs are shown in Fig. 3(a). They indicate significant decrease in the DOS value at the Fermi level in the vicinity of $10\div30\%$ Np concentrations. This drop of DOS manifests itself in the corresponding minimum of the calculated RR curve for Np-Pu alloy that qualitatively reproduces experimental data. With the increase in Pu concentration, the value of alloys DOS at the Fermi level demonstrates a slight modification and the configuration factor $(c_A c_B)$ determines quasiparabolic type of RR concentration dependence in interval $30\div90\%$ Np, see Fig. 4, also in good agreement with available experimental data.

Results of RR calculations (in arbitrary units) for Np-Pu, Np-Am, and Np-Cm alloys are presented in Fig. 4. Note that the RR curves for Np-Am and Np-Cm alloys are similar to the ones obtained earlier in a qualitative consideration of RR,

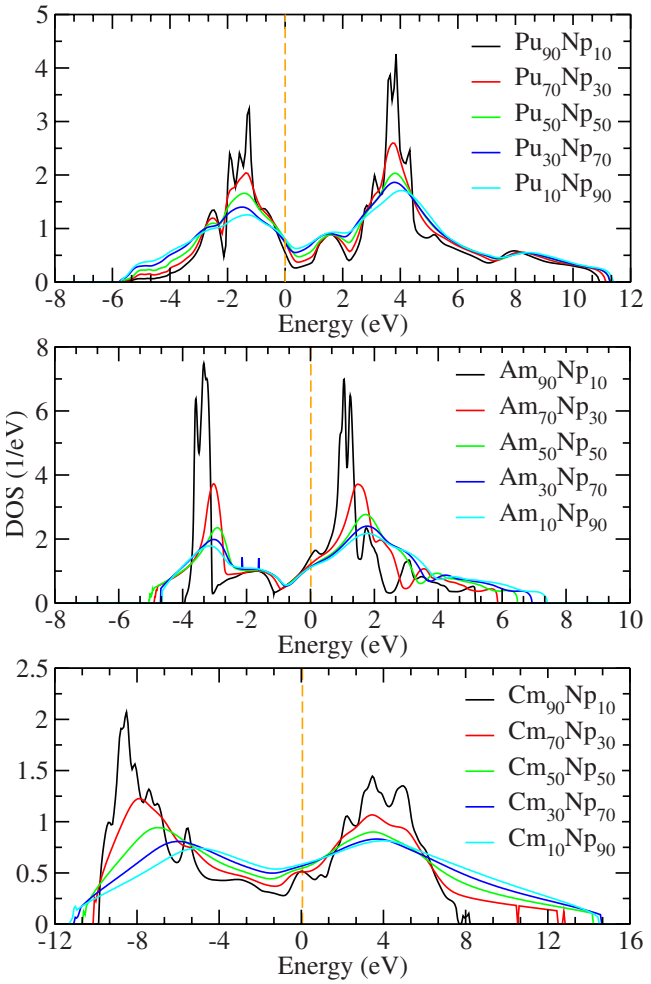

FIG. 3. (Color online) Density of states of Np-Pu, Np-Am, and Np-Cm alloys as a function of compound concentration calculated by the CPA method.

see Fig. 2. The maximum of these curves is significantly shifted from the point of equal concentration. Whereas, despite a local anomaly in the RR curve for Np-Pu alloy, which might be caused by the impurities and radiation damage of

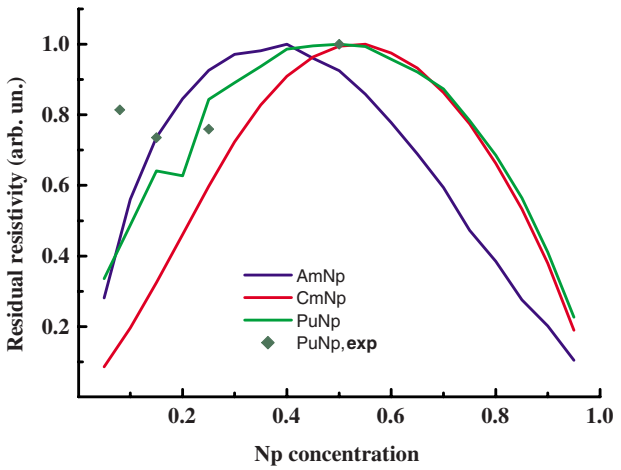

FIG. 4. (Color online) Residual resistivity of Np-Pu, Np-Am, and Np-Cm alloys. Experimental data are taken from Ref. 2.

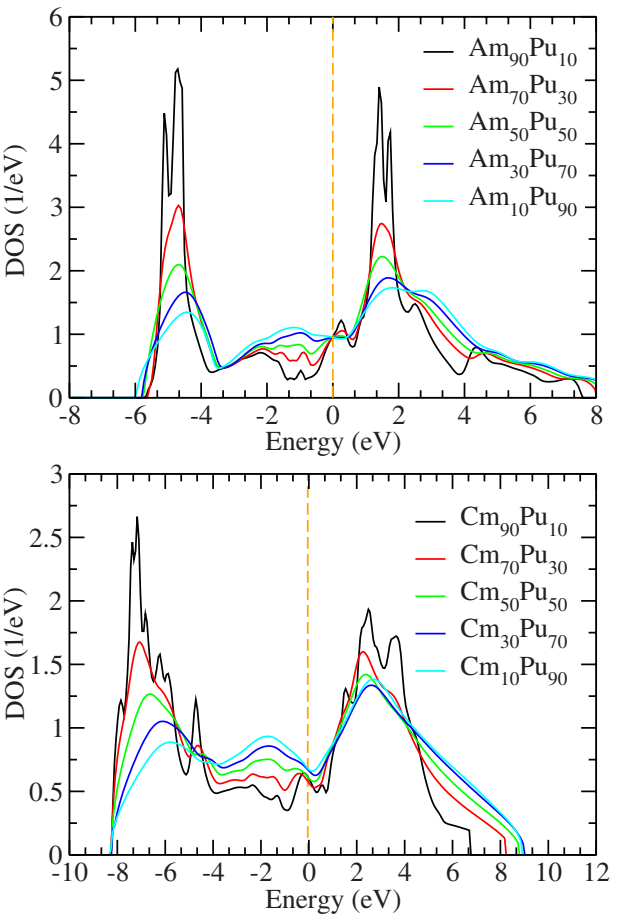

FIG. 5. (Color online) DOS of Am-Pu and Cm-Pu alloys.

the samples,[2] it is even more similar to the Nordgeim parabola, and the position of the RR maximum has a minimal shift from the equal concentration point. These differences originate from the different modification of alloys DOS at the Fermi level with concentration. In all considered alloys quasilinear region of RR concentration dependencies was found in agreement with our previous qualitative result. However, one can see that the evolution of the calculated DOS values at the Fermi level for Np-Am and Np-Cm alloys is not so significant as in Np-Pu case. The former concentration dependencies of RR are close to the ones of ordinary transition-metal alloys.

2. Residual resistivity of Pu-Am and Pu-Cm alloys

The CPA results of the Am-Pu and Cm-Pu alloys DOS calculations are presented in Fig. 5. As in the case of the Np-based alloys, one could conclude that initially localized $j=5/2$ and $j=7/2$ $5f$-electron states are unstable and could easily be destroyed by alloying with another metal. However, in case of Pu-Am alloys, signs of weak localization are preserved in all concentration regions, which qualitatively agrees with the modern photoelectron spectroscopy data.[3] The DOS values at the Fermi level in alloys are changed not drastically, and therefore the RR calculated curves in Fig. 6 are in better agreement with the qualitative results.

Experimental data for concentration dependence of RR for Pu-Am alloys are reported only for several samples with

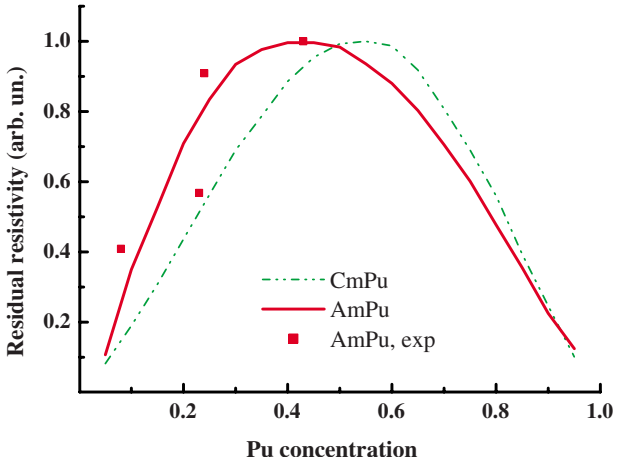

FIG. 6. (Color online) Residual resistivity of Pu-Am and Pu-Cm alloys. Experimental data are taken from Ref. 3.

Am concentration 8, 23, 28, and 43%.[3] One can see that the results of our calculations are in qualitative agreement with the experimental data on average. The deviations from the experimental points could arise from strong modifications of lattice parameter, not taken into account in the CPA calculations. On the other hand, only one point (23%) falls out from a smooth curve that requires additional experimental RR data in this region of concentrations.

Unfortunately, no experimental data are available for Cm-Pu alloys, and hence the presented results Fig. 6 could be considered as a prediction.

3. Residual resistivity of Am-Cm alloys

Our calculations for Am-Cm alloys predict a normal type of RR behavior, see Fig. 7, due to nondrastic changes in DOS values at the Fermi level with concentration, Fig. 8. On the other hand, the RR maximum has significant shift to americium. This feature could be explained if we take into consideration that the value of DOS of Am exceeds the Cm one. The second component reduces the DOS of alloy in such a way that its value at the Fermi level decreases with the decrease in Cm concentration.

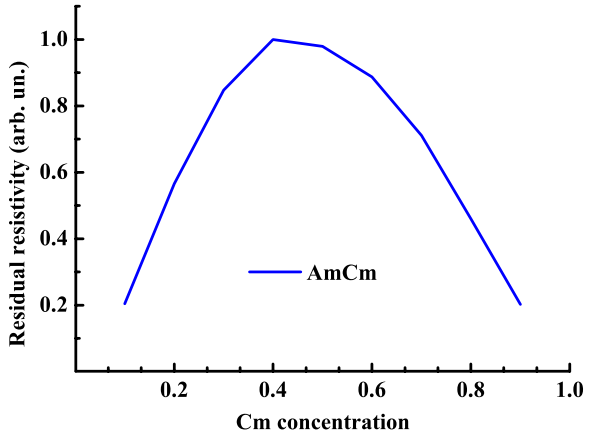

FIG. 7. (Color online) Residual resistivity of Am-Cm alloys.

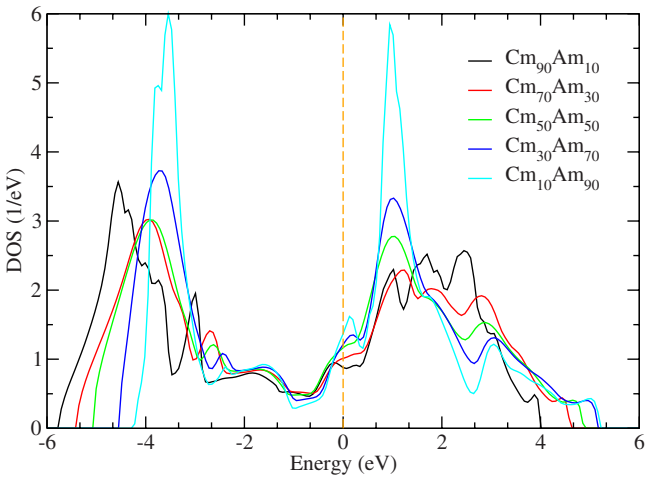

FIG. 8. (Color online) DOS of Am-Cm alloys.

V. CONCLUSION

In this paper the CPA equations for many-band conductivity model were derived. In this derivation we obviate a necessity to use several artificial and debatable models and any assumptions concerning the specificity of DOS near the Fermi level. Also no assumptions on weakness of the interaction were made for RR calculation for all real systems under consideration. Then, in terms of the proper model, some qualitative results for RR concentration dependencies were obtained within the perturbation theory and discussed in detail. Starting from the results of numerical simulations of band structure for bcc-neptunium, fcc-plutonium, americium, and curium, the RR concentration dependence of these metals alloys was analyzed from the most general point of view, in terms of many-band conductivity model. The complex structure of d and f electron DOS and their deformations due to electron-impurity interactions were accounted. Initially localized $j=5/2$ and $j=7/2$ $5f$ electron states of fcc-Pu and Am are unstable and could easily be destroyed by alloying with another metal. The traces of localized electron behavior were obtained only in case of Am-Pu alloys.

Local anomalies of RR in Np-Pu alloys originate from strong modification of DOS value at the Fermi level. Ordinary concentration dependencies of Np-Am and Np-Cm alloys were reproduced numerically. The obtained theoretical results for residual resistivity were compared with a few available experimental data reported in the literature. Good agreement with experiment was found for Np-Pu and Am-Pu alloys. Additional experiments for these alloys are required. Normal type of RR concentration dependencies in Pu-Am, Pu-Cm, and Am-Cm alloys were obtained. No considerable changes in DOS value at the Fermi level were detected in these alloys and hence RR curves have an ordinary behavior. It should be emphasized that the shape of RR curves obtained qualitatively and numerically for real alloys are in general the same.

ACKNOWLEDGMENTS

This research was supported by the Russian Foundation for Basic Research under Projects No. 08-02-99067 and No. 09-02-00431.

*Present address: Institute of Metal Physics, Ural Division of Russian Academy of Sciences, 18 S. Kovalevskaya St., 620041 Ekaterinburg GSP-170, Russia; y.tsiovkin@mail.ustu.ru

[1] A. M. Boring and J. L. Smith, Los Alamos Sci. **26**, 90 (2000); S. S. Hecker and J. C. Martz, *ibid.* **26**, 238 (2000).
[2] C. E. Olsen and R. O. Elliott, Phys. Rev. **139**, A437 (1965).
[3] W. Müller, R. Schenkel, H. E. Schmidt, J. C. Spirlet, D. L. McElroy, R. O. A. Hall, and M. J. Mortimer, J. Low Temp. Phys. **30**, 561 (1978).
[4] N. Baclet, M. Dormeval, L. Havela, J. M. Fournier, C. Valot, F. Wastin, T. Gouder, E. Colineau, C. T. Walker, S. Bremier, C. Apostolidis, and G. H. Lander, Phys. Rev. B **75**, 035101 (2007).
[5] R. Schenkel, Solid State Commun. **23**, 389 (1977).
[6] S. Y. Savrasov, K. Haule, and G. Kotliar, Phys. Rev. Lett. **96**, 036404 (2006), and references therein.
[7] R. Smoluchowski, Phys. Rev. **125**, 1577 (1962).
[8] M. B. Brodsky, Phys. Rev. **137**, A1423 (1965).
[9] A. R. Harvey, M. B. Brodsky, and W. J. Nellis, Phys. Rev. B **7**, 4137 (1973).
[10] M. B. Brodsky, Rep. Prog. Phys. **41**, 1547 (1978).
[11] Yu. Yu. Tsiovkin and L. Yu. Tsiovkina, J. Phys.: Condens. Matter **19**, 056207 (2007).
[12] Yu. Yu. Tsiovkin, M. A. Korotin, A. O. Shorikov, V. I. Anisimov, A. N. Voloshinskii, A. V. Lukoyanov, E. S. Koneva, A. A. Povzner, and M. A. Surin, Phys. Rev. B **76**, 075119 (2007).
[13] N. F. Mott, Adv. Phys. **13**, 325 (1964).
[14] Yu. Yu. Tsiovkin, A. N. Voloshinskii, V. V. Gapontsev, V. V. Ustinov, A. G. Obykhov, A. L. Nikolaev, I. A. Nekrasov, and A. V. Lukoyanov, Phys. Rev. B **72**, 224204 (2005), and references therein.
[15] W. Kohn and L. J. Sham, Phys. Rev. **140**, A1133 (1965).
[16] A. O. Shorikov, A. V. Lukoyanov, M. A. Korotin, and V. I. Anisimov, Phys. Rev. B **72**, 024458 (2005).
[17] A. B. Shick, V. Drchal, and L. Havela, Europhys. Lett. **69**, 588 (2005).
[18] J. H. Shim, K. Haule, and G. Kotliar, Nature (London) **446**, 513 (2007).
[19] V. I. Anisimov, A. O. Shorikov, and J. Kuneš, J. Alloys Compd. **444-445**, 42 (2007).
[20] S. Heathman, R. G. Haire, T. Le Bihan, A. Lindbaum, M. Idiri, P. Normile, S. Li, R. Ahuja, B. Johansson, and G. H. Lander, Science **309**, 110 (2005).
[21] A. Shick, J. Kolorenc, L. Havela, V. Drchal, and Th. Gouder, EPL **77**, 17003 (2007).
[22] P. Söderlind and B. Sadigh, Phys. Rev. Lett. **92**, 185702 (2004).
[23] K. T. Moore, G. van der Laan, R. G. Haire, M. A. Wall, A. J. Schwartz, and P. Söderlind, Phys. Rev. Lett. **98**, 236402 (2007).
[24] A. Landa, P. Söderlind, and A. Ruban, J. Phys.: Condens. Matter **15**, L371 (2003).
[25] S. McCall, M. J. Fluss, B. W. Chung, G. F. Chapline, D. D. Jackson, and M. W. McElfresh, Mater. Res. **893**, 0893-JJ04-03.1 (2006).
[26] L. V. Pourovskii, G. Kotliar, M. I. Katsnelson, and A. I. Lichtenstein, Phys. Rev. B **75**, 235107 (2007).
[27] A. N. Voloshinskii and A. G. Obukhov, Phys. Met. Metallogr. **91**, 238 (2001).
[28] P. Soven, Phys. Rev. **156**, 809 (1967).
[29] A. Lindbaum, S. Heathman, K. Litfin, Y. Méresse, R. G. Haire, T. Le Bihan, and H. Libotte, Phys. Rev. B **63**, 214101 (2001).
[30] W. E. Pickett, S. C. Erwin, and E. C. Ethridge, Phys. Rev. B **58**, 1201 (1998).
[31] *Handbook of Physics and Chemistry*, edited by A. J. Freeman and G. H. Lander (North-Holland, Amsterdam, 1987), Vol. 5.